



Surface characterization and tribological performance of laser shock peened steel surfaces

Arpith Siddaiah, Bo Mao, Yiliang Liao*, Pradeep L. Menezes*

Department of Mechanical Engineering, University of Nevada, Reno, Reno, NV 89557, United States of America

ARTICLE INFO

Keywords:

Laser shock peening
Coefficient of friction
Transfer layer formation
Surface roughness

ABSTRACT

Laser shock peening (LSP) is a preminent surface treatment technique that can surpass many of the modern surface modification processes. Though the wear and surface hardening behavior of the LSP treated surfaces has been extensively investigated, the friction behavior and surface morphological changes due to LSP are not well explored. Hence, the present study focuses on the effect of LSP process parameters on surface morphology and tribological behavior of 1045 steel surfaces. More specifically, the influence of laser intensity on surface roughness and its effect on the coefficient of friction (COF) and transfer layer formation were investigated. The results show that the COF decreased with increasing laser intensity up to a threshold intensity, thereafter, the COF increased with increasing laser intensity. These variation in COF was attributed to the change in surface morphology as a result of applied laser intensity. As the laser intensity increased to a threshold value, the COF decreased as a result of surface strengthening and roughening effects. Beyond the threshold laser intensity, the COF increased as a result of the dominant surface roughening effect.

1. Introduction

Laser shock peening (LSP) is a laser-based surface engineering process, which has been used for widespread industrial applications [1–4]. LSP utilizes laser-induced shock wave to introduce compressive stresses as well as surface hardening effect on the target surface. The basic process of LSP is illustrated in Fig. 1, where the target material is covered with an ablative coating to absorb laser energy. During the LSP process, the laser-matter interaction results in the formation of laser-induced plasma whose expansion is constrained by a transparent confinement. Due to this confinement, a laser-induced shockwave with a high peak pressure (in the order of GPa) propagates into the surface of the target material, leading to an ultrahigh strain rate plastic deformation ($10^5/s$ – $10^6/s$) [2]. As a result, near-surface compressive residual stresses and work-hardened layers are introduced. These surface alterations play an important role in defining the tribological properties of a surface [5–11].

As compared to other surface treatment techniques such as shot peening [12, 13], ultrasonic impact treatment [14, 15], laser surface melting [16, 17], and surface coating deposition [18], LSP provides advantages such as higher flexibility and accuracy, deeper compressive residual stress, and less damage to the initial surface [19, 20]. These characteristics of LSP have encouraged tribologists to envision LSP as a

sustainable surface treatment technique to control the tribological properties of metallic surfaces. The LSP on brass material surface was studied by Wang et al. [21], where it was shown to enhance the microhardness by 28.3% and reduce the wear mass loss by 31.78%. This enhanced microhardness and wear resistance was attributed to the laser beam overlapping ratio which defines a specific peak pressure during LSP. The LSP on 7075-aluminum alloy surface was studied by Wang et al. [22], where the authors concluded that LSP is an effective approach to decrease the depth and width of wear scars, and to reduce the abrasion loss in seawater environment. These observations were attributed to the grain refinement during LSP which increases the surfaces hardness and abrasion resistance. Similarly, the LSP of duplex stainless steel surfaces was studied by Lim et al. [23] where it was shown that a high laser intensity of 10 GW/cm^2 can be used to reduce the wear volume and corrosion in seawater by 39% and 74.2%, respectively. These enhancements were achieved through optimization of LSP process parameters which aided in reducing the number of corrosion pits on the wear track. In another study, the influence of LSP on the wear and degradation performance of AZ31B magnesium alloy surface was investigated by Zhang et al. [11]. Based on the observed changes in surface hardness, it was reported that the LSP increased the yield strength of magnesium alloy surface from 128 to 152 MPa along with significant wear resistance enhancements.

* Corresponding authors.

E-mail addresses: yliiao@unr.edu (Y. Liao), pmenezes@unr.edu (P.L. Menezes).

<https://doi.org/10.1016/j.surfcoat.2018.07.087>

Received 16 March 2018; Received in revised form 27 June 2018; Accepted 30 July 2018

Available online 31 July 2018

0257-8972/ © 2018 Published by Elsevier B.V.

Nomenclature

S_a	3D average roughness amplitude
R_a	2D average roughness amplitude
S_q	3D root mean square roughness amplitude
S_{ku}	3D Kurtosis
S_{sk}	3D Skewness

Although most of tribological studies on LSP have focused on the enhanced surface hardness and wear resistance [8, 24–27], the friction behavior and surface morphological changes due to LSP are not well explored. This might be attributed to the complexity of combined surface strengthening and roughening effects introduced by LSP. The investigations conducted by Petan et al. [28, 29] on the effects of laser intensity and spot size for LSP of maraging steel surface indicate that the LSP performed without an ablative coating can generate a relatively low surface roughness. Investigation conducted by Ren et al. [30] using Ti-6Al-4V alloy shows that LSP with a low laser intensity could reduce the surface roughness considerably. Similarly, Zhang et al. [11] showed that a low laser intensity treatment of AZ31B magnesium alloy surface produces dimple effects with a low average surface roughness as compared to the dimple effects observed at a high laser intensities. These reports have studied the effect of LSP on surface morphology, but there is an insufficient use of surface roughness parameters to define the effect of LSP on surface morphology. Most of these studies consider 2D and 3D surface roughness parameters of average roughness (R_a/S_a), maximum height of the profile (R_z/S_z), and root mean square roughness (R_q/S_q). However, tribological studies concerning surface roughness have shown that different textured surfaces with a similar average surface roughness (R_a) can exhibit varying tribological properties in terms of the COF and the amount of transfer layer formation [31–33]. This indicates that one or two surface roughness parameter are insufficient to quantify the topographical changes observed on a given surface and to describe the functional characteristic like friction [34, 35]. Menezes et al. [34, 36] conducted a series of investigations concerning the influence of surface texture and surface roughness on the COF. In these studies, different surface textures were characterized by 25 roughness parameters including hybrid and non-dimensional roughness parameters. These roughness parameters were then correlated to the friction behavior of the surface textures. It was shown that the variations in COF for different surface textures (with similar surface roughness) was due to dominant influence of plowing component of friction at the asperity contact. Since, the plowing component is defined by the asperity slope on the harder substrate surface it is necessary to study the dominant surface roughness parameters affected by LSP process and its influence on the friction behavior.

The present study aims to characterize the effect of LSP on surface morphology and friction behavior of metallic surfaces, with specific

focus on the influence of laser intensity on surface roughness, coefficient of friction (COF), and transfer layer formation. As a result of this investigation a surface behavior model describing the effect of laser intensity on surface morphology has been developed. The study also demonstrates the use of an effective surface modification technique to control the tribological properties of a surface.

2. Materials and methods

The experimental work design of the current study is schematically represented in Fig. 2. The materials and methods are detailed in this section.

2.1. Materials

High strength 1045 medium carbon steel (ASTM A108) of 30 mm × 12 mm × 10 mm were used as the plate material on which LSP was performed. In order to perform the scratch test on these steel plate surfaces, 6061-T6 aluminum alloy (ASTM B211) of 3 mm diameter was used as the counterpart pin material. The material composition and physical properties of the tribo-pair (pin and plate) is detailed in Table 1. The tribo-pair used in the present study has widespread applications in overhead power lines as Aluminum Conductor Steel-Reinforced cables (ACSR), electrical connectors involving aluminum connections with steel, aircraft fittings, marine fittings and hardware, valves and valve parts.

2.2. LSP of steel surfaces

The initial preparation of the steel surfaces before LSP, involved rough polishing using sand papers of grit sizes 100, 320, 600, 800 and 1200. This was followed by a fine wet polishing using 3 μm, 0.5 μm diamond slurry, and 0.06 μm colloidal silica suspension. Five steel specimen surfaces were polished in this manner to have an average surface roughness (S_a) of $0.1 \pm 0.03 \mu\text{m}$. After the initial surface preparation, the LSP was performed on four steel specimen surfaces at specific laser intensities, as indicated in Table 2. The remaining one untreated steel surface was considered as the reference surface. The LSP was performed using a nanosecond pulsed Nd-YAG laser with a wavelength of 1064 nm and a pulse duration time (t) of 5 ns. The laser beam diameter (d) was maintained at 1.5 mm. A black tape with a thickness of 0.132 μm and BK7 (borosilicate) glass were used as the ablative coating and confinement media, respectively. The black tape was carefully peeled off after processing, and the specimens were cleaned in an ultrasonic cleaner using N-hexane solution to remove the adhesive remnants of the black tape. Further, the specimens were ultrasonically cleaned in soap water and acetone before being stored in a desiccator.

2.3. Surface characterization

The surface topography of each specimen was characterized before and after the LSP using Rtec 3D optical profilometer which has a resolution of 50 nm. As an example, the surface profiles before and after the LSP treatment is shown in Fig. 3. An area of $1.11 \times 0.89 \text{ mm}^2$ was profiled at five random locations on the sample surface and an average of these roughness value has been reported. During this surface characterization, various 3D surface roughness parameters were recorded to investigate the surface morphological changes due to LSP. Further, Vickers microhardness test (HV) was conducted to study the effect of LSP on the surface hardness. The HV values were measured using a diamond tip indenter with a load of 500 g and a dwell time of 10 s. The hardness value of untreated specimen was considered as the baseline, against which the hardness of LSP treated samples were compared and analyzed.

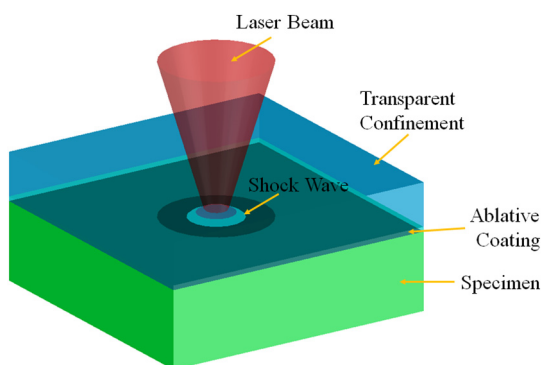


Fig. 1. Schematic of Laser shock peening Process.

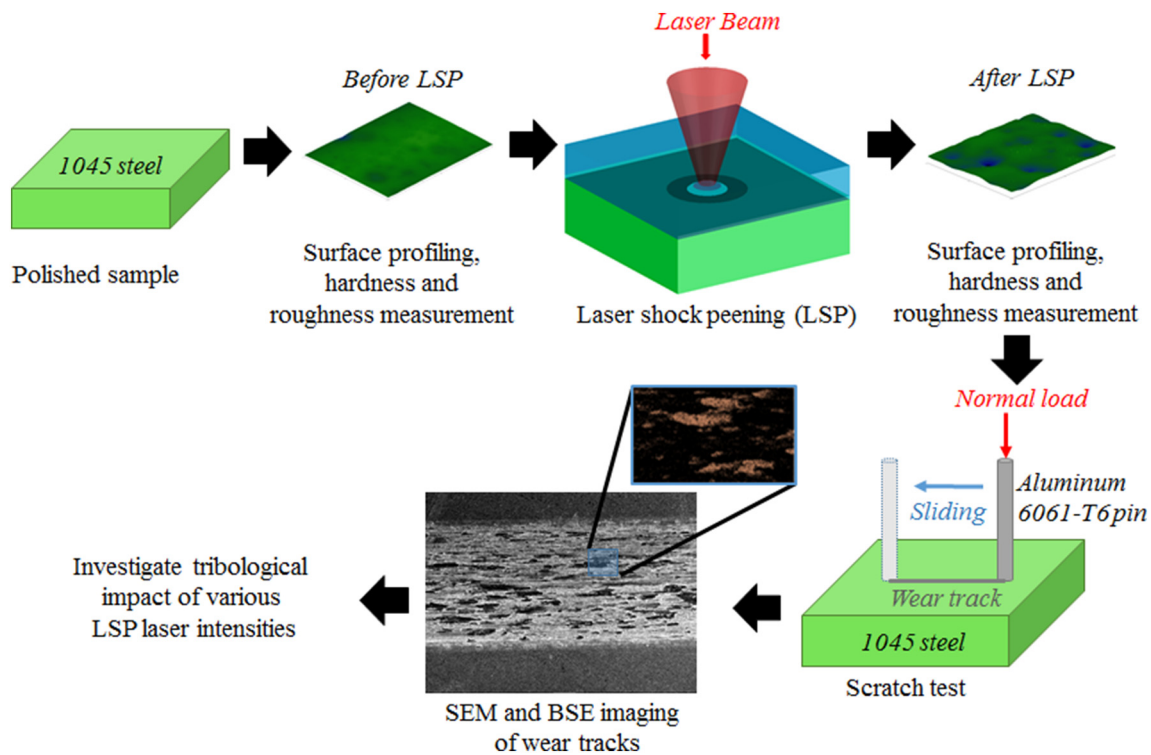


Fig. 2. Experimental work scheme.

Table 1
Material composition and physical properties of 1045 medium carbon steel and 6061-T6 aluminum alloy.

Properties	1045 medium carbon steel (ASTM A108)	6061-T6 aluminum alloy (ASTM B211)
Material composition		Aluminum 95.1–98.2% Chromium 0.4–0.8% Copper 0.05–0.4% Iron 0–0.7% Magnesium 0.8–1.2% Manganese 0–0.15% Nickel 0–0.05% Silicon 0.4–0.8% Titanium 0–0.15% Zinc 0–0.25% Zirconium 0–0.25% Other 0.15%
Iron	98.21–98.85%	
Carbon	0.43–0.50%	
Manganese	0.60–0.90%	
Phosphorus	0–0.04%	
Silicon	0.15–0.30%	
Sulfur	0–0.05%	
Yield strength	530 MPa	241.32 MPa
Hardness	190HV0.5	107HV0.5
Hardness rating	Medium	Soft
Melting point	1427 °C	582.22 °C
Elongation	19%	12.5%

Table 2
LSP process parameters for different specimens.

Specimen number	Laser intensity, I (GW/cm ²)
#1 (untreated)	0
#2	1.68
#3	3.46
#4	4.40
#5	6.00

2.4. Tribological performance

The tribological properties, such as friction, and transfer layer formation were investigated using a scratch test. The scratch tests were performed as per ASTM G133 on each of the five steel surfaces (four

LSP treated and one untreated surfaces) using aluminum alloy pins as shown schematically in Fig. 4. The scratch tests were performed using an Rtec multi-function tribometer 5000 which is equipped with a high-resolution 1D normal force load cell (15 mN resolution) and a 1D friction force load cell (6 mN resolution). The test conditions for the scratch experiments are detailed in Table 3. These test conditions were determined based on previous investigations that considered similar applicability of the steel substrate [37, 38]. Before each test, the pin and steel surface were thoroughly cleaned in an aqueous soap solution followed by ultrasonic cleaning in acetone. The repeatability and consistency of the results was verified by performing each scratch test three times.

After the tests, Scanning electron microscope (SEM) was used to analyze the transfer layer formation on the steel surfaces. Backscattered scanning electron microscopy (BSE) coupled with energy dispersive spectroscopy (EDS) was used to obtain data on the composition of transfer layer formed on the wear tracks. Furthermore, the wear tracks were phase mapped to quantify the amount of aluminum transfer layer formed on the steel surfaces.

3. Results and discussion

3.1. Surface characterization

3.1.1. Surface roughness

The 3D surface roughness profiles were recorded before and after LSP of each steel surface. The roughness parameters of the profile that are discussed in this study have been described in detail by Menezes et al. [39]. The surface roughness parameters discussed in this study are – average surface roughness (R_a , S_a), root mean square surface roughness (R_q , S_q), skewness (R_{sk} , S_{sk}), kurtosis (R_{ku} , S_{ku}), average maximum height of valley depth (R_{vm}) and peak height (R_{pm}), average maximum height of the profile (R_z), average wavelength of the profile (λ_a), and average absolute slope (Δ_a). Among the various surface roughness parameters investigated in the present study, it was found that the skewness (S_{sk}) and the kurtosis (S_{ku}) roughness values were

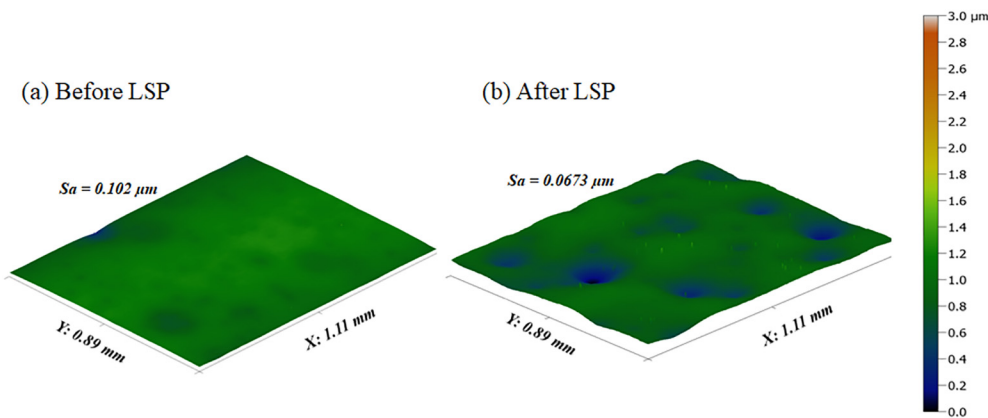


Fig. 3. 3D-Surface topography (a) Before LSP (b) After LSP at I = 1.68 GW/cm².

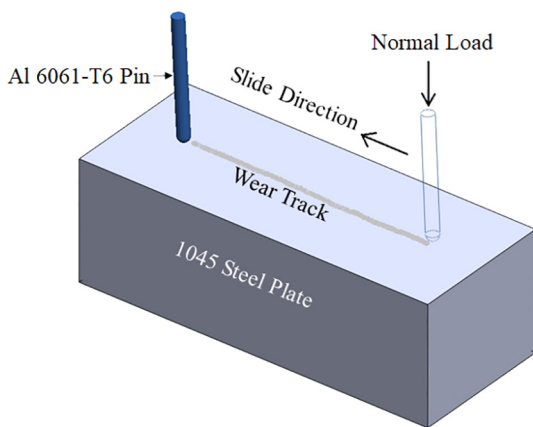


Fig. 4. Schematic diagram of scratch test when Al 6061-T6 pin slides against 1045 steel plate.

Table 3
Scratch test conditions.

Experiment parameters	Values
Specimen surface condition	Dry
Temperature	24 °C
Humidity	30% RH
Load (constant)	50 N
Sliding distance	10 mm
Sliding speed	2 mm/s

significantly affected by the change in laser intensity of the LSP as shown in Fig. 5. The figure shows the observed change in surface roughness amplitudes due to LSP when compared against the most commonly used surface roughness parameters- average surface roughness (S_a) and RMS surface roughness (S_q). It can be observed that as the laser intensity increases, the S_a and S_q show a variation < 0.2, while S_{sk} shows a variation ranging between 0.89 and 2.86 (42.18% to 188%) and S_{ku} shows a variation ranging between 1.9 and 3.32 (61.09% to 92.46%). The S_{sk} and S_{ku} values at each laser intensity of the LSP has been tabulated in Table 4. These variations in 3D roughness values indicate that the traditional methodology of quantifying the changes in surface roughness after the LSP using S_a and S_q [29, 30, 40] is insufficient to describe the changes in surface morphology. It was found that the effect of LSP on surface roughness can be quantified appropriately by using more than one roughness parameter [31, 33, 41, 42]. The roughness parameters S_{sk} and S_{ku} are found to be good representation of the changes in surface roughness as a function of laser intensity.

3.1.2. Surface profile

Investigations were performed to analyze the effect of laser intensity on the surface profile of the LSP treated steel surfaces as shown in Fig. 6. The Fig. 6(a) shows 2D surface profile of the untreated steel surface ($I_1 = 0$ GW/cm²) while the Fig. 6(b)–(e) represent the 2D surface profiles of steel surfaces treated at various laser intensities ($I_2 = 1.68$ GW/cm², $I_3 = 3.46$ GW/cm², $I_4 = 4.4$ GW/cm², and $I_5 = 6.0$ GW/cm²). It can be clearly observed that as the laser intensity increases the asperities are accordingly compressed to be closer to the mean surface line of the profile. This indicates that there is a negative skewing effect on the surface profile as the laser intensity increases. It can be observed in Fig. 6(b) and (c) that for lower intensity treatments a platykurtic form of asperities with low degree of sharpness were formed. Whereas, in case of high laser intensity treatment seen in Fig. 6(d) and (e) symmetric-small sharp asperities were formed. Compared to the untreated surface profile seen in Fig. 6(a) the asperities are observed to undergo a progressively increasing degree of plastic deformation as a function of laser intensity.

The observed changes in the asperity profiles are better understood when analyzed with their respective laser shockwave pressures during the LSP. The laser shockwave pressure as a function of time observed at each laser intensity treatment is shown in Fig. 7. The peak pressures were calculated using the relationship between the laser intensity (I), and the laser shock peak pressure (P) which is expressed as Eq. (1):

$$P = 0.01 \sqrt{(\alpha/2\alpha + 3) \times Z \times I} \tag{1}$$

where α is the efficiency of the interaction, Z is the combined shock

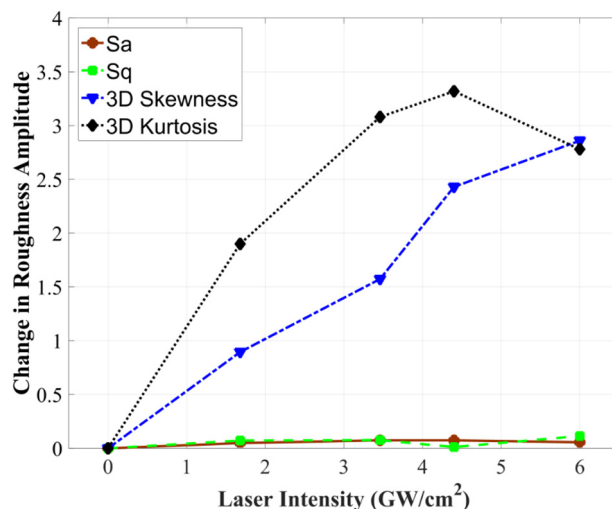


Fig. 5. Change of various roughness parameters as a function of laser intensity.

Table 4
3D Skewness and Kurtosis amplitudes before and after LSP treatment.

Laser intensity (GW/cm ²)	3D Skewness (S _{sk})			3D Kurtosis (S _{ku})		
	Before LSP	After LSP	Change due to LSP	Before LSP	After LSP	Change due to LSP
I ₁ = 0	-1.22	-1.22	0.00	3.08	3.08	0
I ₂ = 1.68	-2.11	-1.21	0.89	3.11	1.21	1.90
I ₃ = 3.46	-1.80	-0.22	1.57	3.67	0.59	3.08
I ₄ = 4.40	-2.08	0.34	2.43	3.58	0.26	3.31
I ₅ = 6.00	-1.52	0.76	2.86	3.59	0.81	2.78

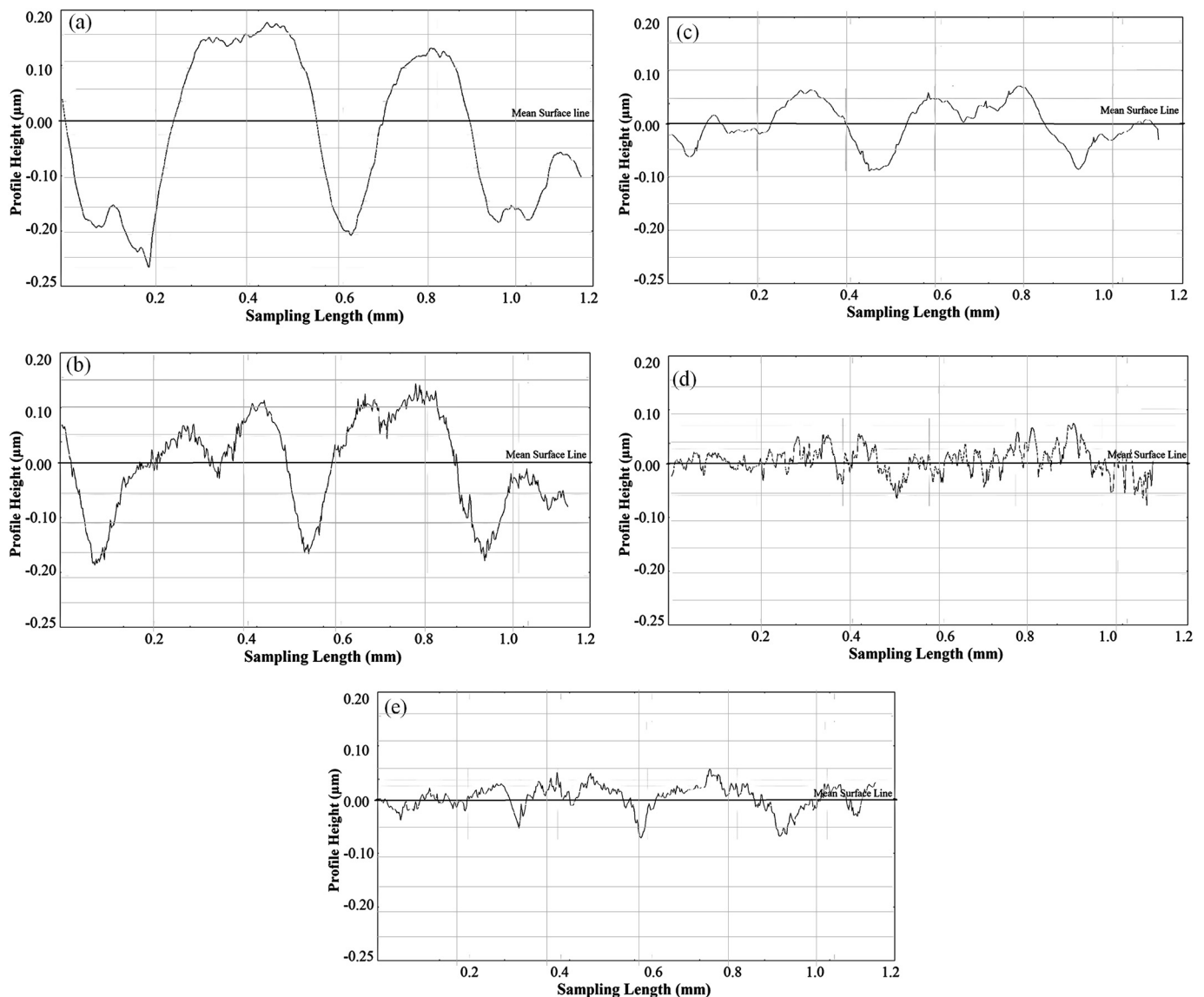


Fig. 6. Effect of laser intensity on surface profile: (a) Untreated Surface (I₁ = 0 GW/cm²) (b) LSP at I₂ = 1.68 GW/cm² (c) LSP at I₃ = 3.46 GW/cm² (d) LSP at I₄ = 4.4 GW/cm² (e) LSP at I₅ = 6.0 GW/cm².

impedance defined as Eq. (2):

$$Z = 2 / ((1/Z_1) + (1/Z_2)) \tag{2}$$

where Z₁ and Z₂ are the shock impedance of the material and the confining media, respectively. The estimations shown in Fig. 7 are based on the well-accepted LSP model proposed by Fabbro et al. [43]. It can be observed that as the laser intensity is increased from 1.68 to 6.0 GW/cm², the laser shockwave peak pressure increases from 2.9 to 5.6 GPa. This laser shockwave pressure introduces a compressive

loading effect on the asperities leading to the observed surface plastic deformation. The gradient of asperity restructuring at various laser intensities can be attributed to the magnitude of laser shock loading during the LSP. At low laser intensity treatments there was a low gradient of the shockwave pressure that generated asperities with platykurtic form of peaks having low sharpness. Whereas, at high laser intensities a larger gradient of the shockwave pressure was observed resulting in high degree of surface plastic deformation that generates sharp asperities [28].

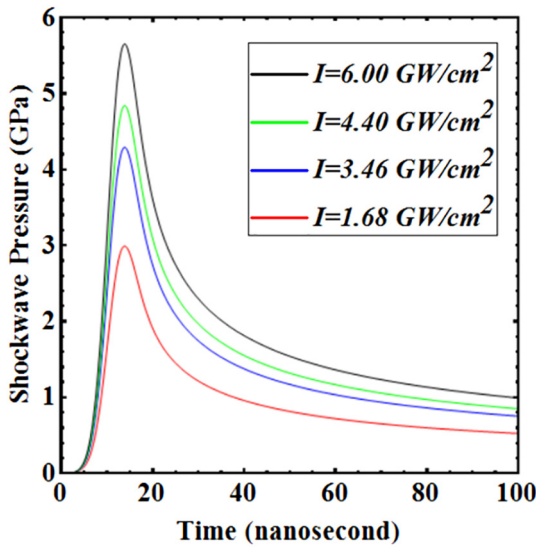


Fig. 7. Laser shockwave pressure as a function of time with respect to different laser intensities.

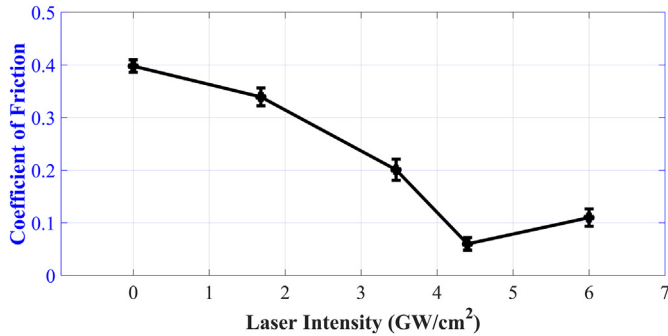


Fig. 8. Effect of laser intensity on coefficient of friction.

Table 5
Comparison of coefficient of friction values before and after LSP treatments.

Materials	LSP parameters	COF before LSP	COF after LSP	Reference
Ti6Al4V	4.25 GW/cm ²	0.435	0.451	[46]
Ti6Al4V	10 W, 5 mm/s	0.92	0.22	[47]
Al 6061-T6	5.3 GW/cm ²	1.0	1.3	[48]
100Cr6 rolling steel	5.5 GW/cm ²	0.55	0.45	[10]
AISI 1045 steel	4.4 GW/cm ²	0.40	0.067	Present work
	6.0 GW/cm ²	0.40	0.12	

3.2. Tribological performance

3.2.1. Friction behavior

The effect of LSP on the COF is shown in Fig. 8. It can be observed that as the laser intensity increases there is a decrease in the COF. The untreated steel surface exhibits a COF of 0.4 and as the laser intensity increases to 4.4 GW/cm² the COF decreases to 0.067. Upon further increasing the laser intensity to 6.0 GW/cm², the magnitude of COF increases to 0.112. Depending on the applied laser intensity the COF can be reduced by 17.5%–83.25% with reference to the untreated steel surface. This decrease in the COF due to LSP can be attributed to the changes in surface morphology discussed in Section 3.2. As observed in Fig. 6, the process of LSP causes deformation and restructuring of the asperities depending on the applied laser intensity. Fig. 6(a) which corresponds to the untreated steel surface exhibits a COF of 0.4 and when the surface was treated with a laser intensity of 1.68 GW/cm² the COF decreased by 17.5%. This can be attributed to the plastic deformation of asperities due to LSP which results in smaller peaks and valleys as compared to the untreated steel surface. In a similar manner, as the laser intensity was further increased to 3.46 GW/cm² (Fig. 6(c)) and 4.4 GW/cm² (Fig. 6(d)) the asperity size decreased to create a surface of platykurtic form with low sharpness. At these two laser intensity treatments the COF was observed to decrease by 50% and 83.25%, respectively. It is also important to note that as the laser intensity increased there was a decrease in the peak-valley distance relative to the mean surface line and this distance was minimal when treated at 4.4 GW/cm². Similar effects of LSP have been indicated by Prabhakaran et al. [44] and Trdan et al. [45].

Further, when the laser intensity was increased to 6.0 GW/cm² the COF was found to increase to a value of 0.112 as compared to a COF of 0.067 at 4.4 GW/cm². This change in the COF can be attributed to the change in surface morphology from a valley dominant profile to a peak dominant profile with small asperities (Fig. 6(e)). It can be observed that more sharp peaks are formed due to the high-density plastic deformation of asperities during LSP at 6.0 GW/cm². This observation corresponds to the change in kurtosis values for the surface treated at 6.0 GW/cm² as seen in Table 4. The surface treated at 6.0 GW/cm² exhibits a higher kurtosis value of 0.81 as compared to 0.26 for 4.4 GW/cm².

The observed trend in COF as a function of laser intensity indicates that the COF for a given surface can be precisely varied using LSP. In order to understand the relevance of the observed change in COF, the results from the present study have been compared with other similar studies and is shown in Table 5 [10, 46–48]. It is to be noted that, even though similar laser intensity treatments have been considered in these studies, the material properties and tribological test parameters (such as, load, velocity, and surface roughness) are different. It is also important to note that the other studies listed in Table 5 did not consider the effect of surface morphology on the COF. The present work was able to achieve the lowest COF when the 1045 steel surface was treated at



Fig. 9. Wear track on steel surfaces treated at various laser intensities.

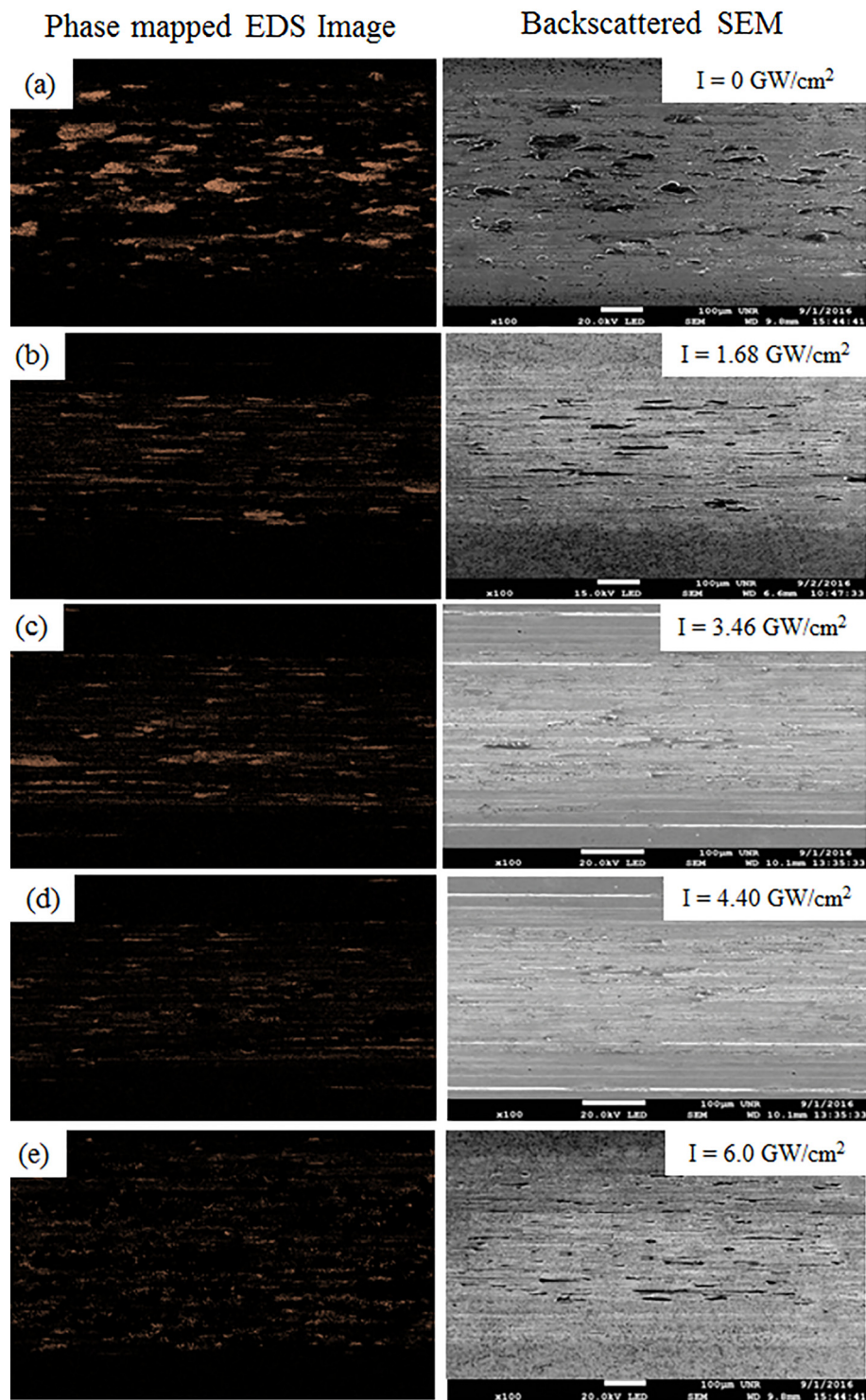


Fig. 10. SEM backscattered images coupled with phase mapped EDS images of Al transfer layer formed on Laser Shock Peened surfaces at laser intensities of (a) $I = 0 \text{ GW/cm}^2$ (untreated surface); (b) $I = 1.68 \text{ GW/cm}^2$; (c) $I = 3.46 \text{ GW/cm}^2$; (d) $I = 4.4 \text{ GW/cm}^2$; (e) $I = 6 \text{ GW/cm}^2$.

laser intensities of 4.4 and 6.0 GW/cm^2 . This study demonstrates that it is possible to identify an optimum laser intensity which would produce a surface morphology that exhibits a low COF during sliding. Hence, it is necessary to consider the effect of surface morphology in defining the tribological behavior of LSP surfaces.

3.2.2. Transfer layer formation

The wear tracks observed after the scratch tests at various laser intensities are shown in Fig. 9. These wear tracks were analyzed under

SEM to investigate the morphology of transfer layer formation. The BSE coupled with phase mapped EDS images of wear tracks are shown in Fig. 10. The figure shows aluminum transfer layer formed during scratch test along the wear tracks. It can be observed that as laser intensity increases there is a significant reduction in the amount of transfer layer formed on the wear tracks. Though, Fig. 10 represents a small section of the wear track, phase mapping was performed on the entire length of the wear track to quantify the exact amount of aluminum transfer layer. The observed trend in transfer layer formation

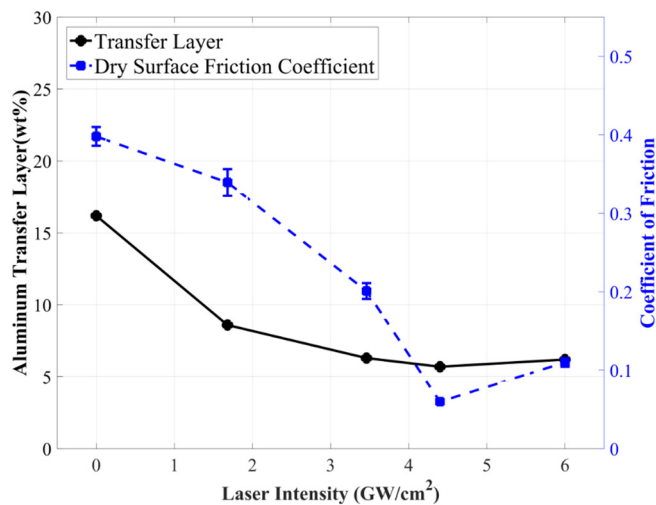


Fig. 11. Effect of LSP on weight percentage of Al transfer layer formation compared with COF.

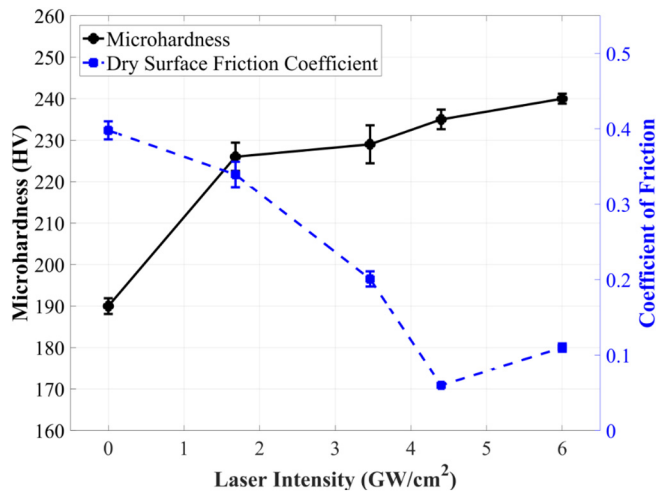


Fig. 12. Effect of LSP on surface hardness compared with COF.

was compared with the corresponding COF values and laser intensities as shown in Fig. 11. It can be observed that the weight percentage of aluminum transfer layer as a function of laser intensity exhibits a similar trend as the COF. This indicates that the change in surface morphology due to LSP not only decreases the COF but also reduces the amount of transfer layer formed on the steel surfaces. The untreated steel surface exhibits a transfer layer of 17% and as the laser intensity increases to 4.4 GW/cm² the transfer layer decreases to 5.4%. This is due to the small asperities formed during LSP at 4.4 GW/cm² which reduces the amount of shear stresses experienced by the asperities at the tribo-pair interface. This in-turn results in low weight percentage of transfer layer formation. Upon further increasing the laser intensity to 6.0 GW/cm², the transfer layer increases slightly, to 6.5%. At this laser intensity, small asperities with sharp peaks can be observed which increases the plowing effect by the asperities at the contact interface and thus increases the transfer layer formation. It can also be inferred that the same mechanism lead to a 67.2% increase in the COF at LSP of 6.0 GW/cm² as compared to the COF at 4.4 GW/cm².

3.2.3. Surface hardness

Microhardness tests were carried out on LSP surfaces to investigate the surface strengthening effect by the LSP. It was found that the surface hardness increases progressively with laser intensity as shown in Fig. 12. This is mainly attributed to the strain hardening effect

introduced by the LSP [24–27]. Even though it is intrinsic for the COF to decrease as the hardness of the surface increases, an 83.25% drop in COF cannot be attributed only to the change in surface hardness. It can be observed in Fig. 12 that when the laser intensity was increased from 0 to 1.68 GW/cm², the COF decreased from 0.4 to 0.33 (17.5% decrease) with an increase in the surface hardness from 190 to 225 HV (18.4% increase). Increasing the laser intensity from 1.68 GW/cm² to 4.4 GW/cm² lead to a decrease in COF from 0.33 to 0.067 (79.7% decrease) and an increase in the surface hardness from 225 to 234 HV (4% increase). When the laser intensity was further increased from 4.4 GW/cm² to 6.0 GW/cm², the COF increased from 0.067 to 0.112 (67.2% increase), respectively. Additionally, for the same increase in laser intensity (4.4 GW/cm² to 6.0 GW/cm²) the surface hardness increased by only 4 HV (1.71% increase), which is negligible as compared to the observed increase in COF. This indicates a dominant effect of the surface roughening at higher laser intensities. Similar roughening effects at high laser intensity treatments have been recently reported [44]. These results indicate that for a low laser intensity range of LSP, both surface strengthening and roughening effects contribute to the decrease in COF. Whereas, for a high laser intensity range of LSP, the surface strengthening effect reaches a saturation point and the surface roughening will have a dominant effect on the COF.

3.3. Surface behavior model

The effect of laser intensity on the surface profile as shown in Fig. 6 indicated that the surface morphology varies with laser intensity. Additionally, the formation of transfer layer during sliding also varied as a function of the applied laser intensity (Fig. 10). Based on these findings and the observed COF, a surface behavior model for LSP treated surfaces was developed as shown in Fig. 13. The model represents a direct proportionality between the laser intensity and change in surface morphology due to plastic deformation of asperities. At low laser intensities, the asperity peaks were found to be plastically deformed (“squashed”) reducing the overall kurtosis (sharpness) of the surface profile. As a result, the surface experienced a lower shear force during sliding leading to a 17.5% decrease in COF as compared to the untreated surface. When the surface was treated at an optimum laser intensity the asperities undergo plastic deformation to yield a profile with minimum kurtosis and skewness. This optimum change in surface morphology minimizes the shear force during sliding providing an 83.5% decrease in COF as compared to the untreated surface. At high laser intensities, the asperities undergo extreme plastic deformation leading to restructuring of the asperities. This results in small-sharp asperities on the surface. Even though, the surfaces treated at high and optimum laser intensities experience a low shear force due to small asperities, the sharp asperities on surface treated at high laser intensity lead to a 67.2% increase in COF as compared to the surface treated at optimum laser intensity. This can be attributed to the increase in plowing effect as a result of the sharp asperities on the surfaces treated at high laser intensities. The high laser intensity treated surface can still provide a 72% decrease in COF as compared to the untreated surface. *This behavior of friction with respect to the laser intensity and surface morphology indicates that COF can be controlled using appropriate laser intensity to suitably modify the surface morphology.*

The present study shows that LSP can be used as an effective surface modification tool to enhance not only the wear resistance and surface hardness but also to control the friction behavior of the surface. The study also shows that a fundamental understanding of the friction behavior and surface morphology for LSP treated surface is necessary to maximize the effectiveness of the surface modification technique.

4. Conclusions

The present study aimed to investigating the effects of LSP on the tribological properties of the steel surfaces. More specifically, the study

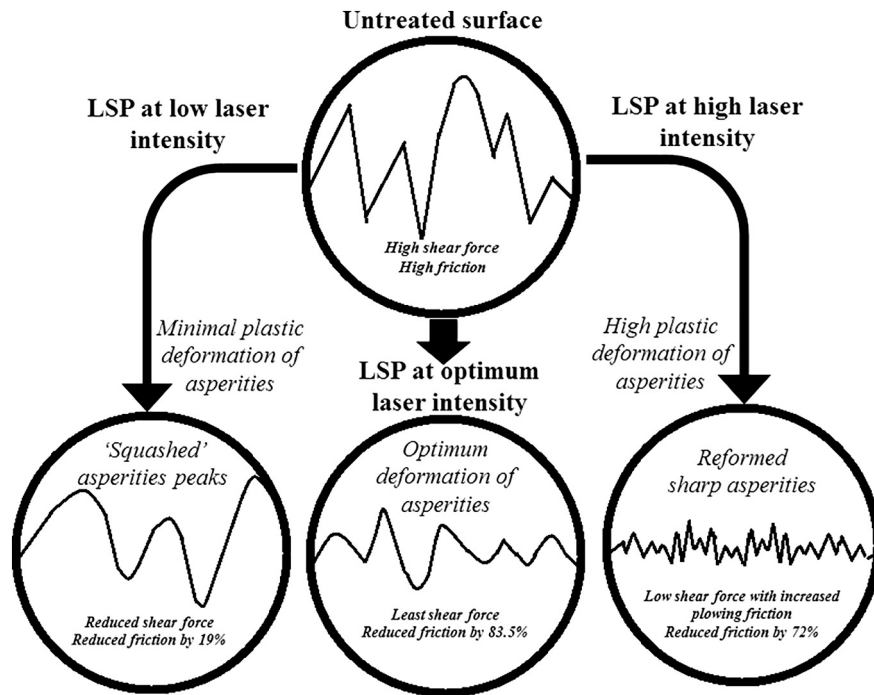


Fig. 13. Surface texture model for laser shock peening at various laser intensities.

investigated the effects of laser intensity on the surface roughness, surface profile, COF, transfer layer formation, and surface hardness. The study also investigated the interdependency of surface morphology and COF followed by interdependency of surface morphology and surface hardness to clearly discern the effects of LSP. Some of the major findings of the study are as follows:

- The roughness parameters S_{sk} and S_{ku} were found to be good representations of the changes in surface roughness as a function of laser intensity.
- The gradient of restructuring the asperities at various laser intensities was attributed to the magnitude of laser shock loading during LSP.
- At low laser intensity treatments there was a low gradient of the shockwave pressure that generated asperities with platykurtic form of peaks having low sharpness. Whereas, at high laser intensities a larger gradient of the shockwave pressure was observed resulting in high degree of surface plastic deformation with sharp asperities.
- Depending on the applied laser intensity the COF can be reduced by a range of 17.5% - 83.25% with reference to the untreated steel surface.
- The change in surface morphology due to LSP not only decreases the COF but also reduces the amount of transfer layer formed on the steel surface.
- The aluminum transfer layer formation as a function of laser intensity exhibits a similar trend as the COF.
- The observed trend in COF as a function of laser intensity indicates that the COF for a given surface can be precisely varied using LSP.
- For a low laser intensity range of LSP, both surface strengthening and roughening effects contribute to the decrease in COF.
- For a high laser intensity range of LSP, the surface strengthening effect reaches a saturation point and the surface roughening will have the dominant effect on the COF.

Acknowledgement

The authors appreciate the financial support by startup funding from the Department of Mechanical Engineering at the University of

Nevada, Reno. Y. Liao appreciates the support by ORAU Ralph E. Powe Junior Faculty Enhancement Award, 2016.

References

- [1] B.P. Fairand, A.H. Clauer, Laser generation of high-amplitude stress waves in materials, *J. Appl. Phys.* 50 (3) (1979) 1497–1502.
- [2] A.H. Clauer, B.P. Fairand, Interaction of laser-induced stress waves with metals, in: E. Metzbowser (Ed.), *Applications of Lasers in Materials Processing*, E. Metzbowser, ed., ASM International, Proceedings of the Conference, Washington, D.C., USA, April 18–20, 1979, pp. 291–315.
- [3] B. Ahmad, M.E. Fitzpatrick, The effect of laser shock peening on hardness and microstructure in a welded marine steel, *J. Eng.* 2015 (13) (2015) 115–125 *Institution of Engineering and Technology*.
- [4] P. Peyre, R. Fabbro, Laser shock processing: a review of the physics and applications, *Opt. Quant. Electron.* 27 (12) (1995) 1213–1229.
- [5] B.P. Fairand, B.A. Wilcox, W.J. Gallagher, D.N. Williams, Laser shock-induced microstructural and mechanical property changes in 7075 aluminum, *J. Appl. Phys.* 43 (9) (1972) 3893–3895.
- [6] A. Clauer, B. Fairand, B. Wilcox, Pulsed laser induced deformation in an Fe-3 Wt Pct Si alloy, *Metall. Trans. A.* 8 (1) (1977) 119–125.
- [7] A.H. Clauer, B.P. Fairand, B.A. Wilcox, Laser shock hardening of weld zones in aluminum alloys, *Metall. Trans. A.* 8 (12) (1977) 1871–1876.
- [8] C.S. Montross, T. Wei, L. Ye, G. Clark, Y.-W. Mai, Laser shock processing and its effects on microstructure and properties of metal alloys: a review, *Int. J. Fatigue* 24 (10) (2002) 1021–1036.
- [9] P. Peyre, R. Fabbro, P. Merrien, H.P. Lieurade, Laser shock processing of aluminium alloys. Application to high cycle fatigue behaviour, *Mater. Sci. Eng. A* 210 (1) (1996) 102–113.
- [10] I. Yakimets, C. Richard, G. Béranger, P. Peyre, Laser peening processing effect on mechanical and tribological properties of rolling steel 100Cr6, *Wear* 256 (3–4) (2004) 311–320.
- [11] R. Zhang, X. Hou, X. Zhou, H. Gao, S. Mankoci, H. Qin, Z. Ren, G.L. Doll, A. Martini, Y. Dong, N. Sahai, C. Ye, Effects of laser shock peening on the wear and degradation behaviors of magnesium alloys, *ASME 2016 11th International Manufacturing Science and Engineering Conference*, Blacksburg, Virginia 24060, USA, June 27–July 1, vol. 2, 2016 (pp. V002T001A005).
- [12] M. Matsui, H. Kakishima, Improvement of tribological performance of steel by solid lubricant shot-peening in dry rolling/sliding contact wear tests, *Wear* 260 (6) (2006) 669–673.
- [13] D. Adamović, M. Babic, B. Jeremic, Shot Peening, Influence on Tribological, Characteristics of Surfaces, *ICSP-7*, Warsaw, Poland, 1999, pp. 350–358.
- [14] A. Amanov, O.V. Penkov, Y.-S. Pyun, D.-E. Kim, Effects of ultrasonic nanocrystalline surface modification on the tribological properties of AZ91D magnesium alloy, *Tribol. Int.* 54 (2012) 106–113.
- [15] A. Amanov, Y.-S. Pyun, S. Sasaki, Effects of ultrasonic nanocrystalline surface modification (UNSM) technique on the tribological behavior of sintered Cu-based alloy, *Tribol. Int.* 72 (2014) 187–197.

- [16] L. Avril, B. Courant, J.J. Hantzpergue, Tribological performance of α -Fe(Cr)-Fe₂B-FeB and α -Fe(Cr)-h-BN coatings obtained by laser melting, *Wear* 260 (4) (2006) 351–360.
- [17] J. Dutta Majumdar, R. Galun, B.L. Mordike, I. Manna, Effect of laser surface melting on corrosion and wear resistance of a commercial magnesium alloy, *Mater. Sci. Eng. A* 361 (1) (2003) 119–129.
- [18] V. Totolin, M. Rodríguez Ripoll, M. Jech, B. Podgornik, Enhanced tribological performance of tungsten carbide functionalized surfaces via in-situ formation of low-friction tribofilms, *Tribol. Int.* 94 (2016) 269–278.
- [19] B. Mao, A. Siddaiah, P.L. Menezes, Y. Liao, Surface texturing by indirect laser shock surface patterning for manipulated friction coefficient, *J. Mater. Process. Technol.* 257 (2018) 227–233.
- [20] K.A. Gujba, M. Medraj, Laser peening process and its impact on materials properties in comparison with shot peening and ultrasonic impact peening, *Materials* 7 (12) (2014).
- [21] F. Wang, Z. Yao, Q. Deng, Experimental study on laser shock processing of brass, *J. Univ. Sci. Technol. Beijing Miner. Metall. Mater.* 14 (6) (2007) 529–532.
- [22] H. Wang, C. Ning, Y. Huang, Z. Cao, X. Chen, W. Zhang, Improvement of abrasion resistance in artificial seawater and corrosion resistance in NaCl solution of 7075 aluminum alloy processed by laser shock peening, *Opt. Lasers Eng.* 90 (2017) 179–185.
- [23] H. Lim, P. Kim, H. Jeong, S. Jeong, Enhancement of abrasion and corrosion resistance of duplex stainless steel by laser shock peening, *J. Mater. Process. Technol.* 212 (6) (2012) 1347–1354.
- [24] P. Shukla, S. Nath, G. Wang, X. Shen, J. Lawrence, Surface property modifications of silicon carbide ceramic following laser shock peening, *J. Eur. Ceram. Soc.* 37 (9) (2017) 3027–3038.
- [25] J.Z. Lu, L.J. Wu, G.F. Sun, K.Y. Luo, Y.K. Zhang, J. Cai, C.Y. Cui, X.M. Luo, Microstructural response and grain refinement mechanism of commercially pure titanium subjected to multiple laser shock peening impacts, *Acta Mater.* 127 (2017) 252–266.
- [26] A. Kulkarni, S. Chettri, S. Prabhakaran, S. Kalainathan, Effect of laser shock peening without coating on surface morphology and mechanical properties of nickel-200, *Mech. Mater. Sci. Eng. J.* 9 (2) (2017) 374–379 Open Access.
- [27] R.K. Nalla, I. Altenberger, U. Noster, G.Y. Liu, B. Scholtes, R.O. Ritchie, On the influence of mechanical surface treatments—deep rolling and laser shock peening—on the fatigue behavior of Ti-6Al-4V at ambient and elevated temperatures, *Mater. Sci. Eng. A* 355 (1) (2003) 216–230.
- [28] L. Petan, J.L. Ocaña, J. Grum, Effects of laser shock peening on the surface integrity of 18% Ni maraging steel, *Stroj Vestn-J Mech E* 62 (2016) (2016) 291–298 5.
- [29] L. Petan, J.L. Ocaña, J. Grum, Influence of laser shock peening pulse density and spot size on the surface integrity of X2NiCoMo18-9-5 maraging steel, *Surf. Coat. Technol.* 307 (2016) 262–270 Part A.
- [30] X.D. Ren, W.F. Zhou, F.F. Liu, Y.P. Ren, S.Q. Yuan, N.F. Ren, S.D. Xu, T. Yang, Microstructure evolution and grain refinement of Ti-6Al-4V alloy by laser shock processing, *Appl. Surf. Sci.* 363 (2016) 44–49.
- [31] P.L. Menezes, Kishore, And Kailas, S. V., Effect of surface roughness parameters and surface texture on friction and transfer layer formation in tin-steel tribo-system, *J. Mater. Process. Technol.* 208 (1–3) (2008) 372–382.
- [32] P.L. Menezes, Kishore, And Kailas, S. V., Influence of roughness parameters and surface texture on friction during sliding of pure lead over 080 M40 steel, *Int. J. Adv. Manuf. Technol.* 43 (7) (2008) 731–743.
- [33] P.L. Menezes, Kishore, S.V. Kailas, Influence of roughness parameters on coefficient of friction under lubricated conditions, *Sadhana* 33 (3) (2008) 181–190.
- [34] P.L. Menezes, Kishore, S.V. Kailas, Influence of surface texture and roughness parameters on friction and transfer layer formation during sliding of aluminium pin on steel plate, *Wear* 267 (9–10) (2009) 1534–1549.
- [35] J. Lundberg, Influence of surface roughness on normal-sliding lubrication, *Tribol. Int.* 28 (5) (1995) 317–322.
- [36] P.L. Menezes, Kishore, S.V. Kailas, On the effect of surface texture on friction and transfer layer formation—a study using Al and steel pair, *Wear* 265 (11–12) (2008) 1655–1669.
- [37] J.J. Coronado, Abrasive size effect on friction coefficient of AISI 1045 steel and 6061-T6 aluminium alloy in two-body abrasive wear, *Tribol. Lett.* 60 (3) (2015) 40.
- [38] X. Zhao, J. Liu, B. Zhu, Z. Luo, H. Miao, Effects of lubricants on friction and wear of Ti(CN)1045 steel sliding pairs, *Tribol. Int.* 30 (3) (1997) 177–182.
- [39] P.L. Menezes, S.V. Kailas, M.R. Lovell, Part I: Chapter-1, “Fundamentals of engineering surfaces”, in: P.L. Menezes, S.P. Ingole, M. Nosonovsky, S.V. Kailas, M.R. Lovell (Eds.), *Tribology For Scientists and Engineers*, Springer-Verlag, New York, 2013, pp. 9–28.
- [40] F.Z. Dai, Z.D. Zhang, J.Z. Zhou, J.Z. Lu, Y.K. Zhang, Analysis of surface roughness at overlapping laser shock peening, *Surf. Rev. Lett.* 23 (03) (2016) 1650012.
- [41] P.L. Menezes, S.V. Kailas, Role of surface texture and roughness parameters on friction and transfer film formation when UHMWPE sliding against steel, *Biosurf. Biotribol.* 2 (1) (2016) 1–10.
- [42] P.L. Menezes, Kishore, S.V. Kailas, Effect of roughness parameter and grinding angle on coefficient of friction when sliding of Al–Mg Alloy over EN8 steel, *J. Tribol.* 128 (4) (2006) 697–704.
- [43] R. Fabbro, J. Fournier, P. Ballard, D. Devaux, J. Virmont, Physical study of laser-produced plasma in confined geometry, *J. Appl. Phys.* 68 (2) (1990) 775–784.
- [44] S. Prabhakaran, A. Kulkarni, G. Vasanth, S. Kalainathan, P. Shukla, V.K. Vasudevan, Laser shock peening without coating induced residual stress distribution, wettability characteristics and enhanced pitting corrosion resistance of austenitic stainless steel, *Appl. Surf. Sci.* 428 (2018) 17–30.
- [45] U. Trdan, J.A. Porro, J.L. Ocaña, J. Grum, Laser shock peening without absorbent coating (LSPwC) effect on 3D surface topography and mechanical properties of 6082-T651 Al alloy, *Surf. Coat. Technol.* 208 (2012) 109–116.
- [46] F.Z. Dai, J. Geng, W.S. Tan, X.D. Ren, J.Z. Lu, S. Huang, Friction and wear on laser textured Ti6Al4V surface subjected to laser shock peening with contacting foil, *Opt. Laser Technol.* 103 (2018) 142–150.
- [47] T. Hu, L. Hu, Q. Ding, Effective solution for the tribological problems of Ti-6Al-4V: combination of laser surface texturing and solid lubricant film, *Surf. Coat. Technol.* 206 (24) (2012) 5060–5066.
- [48] U. Sánchez-Santana, C. Rubio-González, G. Gomez-Rosas, J.L. Ocaña, C. Molpeceres, J. Porro, M. Morales, Wear and friction of 6061-T6 aluminum alloy treated by laser shock processing, *Wear* 260 (7) (2006) 847–854.